Journal of Inclusion Phenomena and Macrocyclic Chemistry (2006) 54: 67–76
DOI 10.1007/s10847-005-4559-1

Interactions of Tetrakis(4-sulfonatophenyl)porphyrin with γ-Cyclodextrin and Alkyltrimethylammonium Bromides in Aqueous Solutions

SANYO HAMAI*, YASUHIRO SASAKI, TAKAHIRO HORI and AIKO TAKAHASHI
Department of Chemistry, Faculty of Education and Human Studies, Akita University, Tegata Gakuen-machi 1-1, 010-8502, Akita, Japan

(Received: 21 October 2004; in final form: 25 March 2005)

Key words: capillary electrophoresis, γ-cyclodextrin, electronic absorption, fluorescence, hexyltrimethylammonium bromide, inclusion complexes, octyltrimethylammonium bromide, tetrakis (4-sulfonatophenyl)porphyrin

Abstract

Tetrakis(4-sulfonatophenyl)porphyrin (TSPP) forms complexes with octyltrimethylammonium bromide (OTMA) and hexyltrimethylammonium bromide (HTMA) in pH 7.3 buffers. At low concentrations of OTMA (HTMA), a 1:1 TSPP–OTMA (HTMA) complex is formed. As the OTMA (HTMA) concentration is increased, a 1:2 TSPP–OTMA (HTMA) complex is also formed. The equilibrium constants for the formation of the TSPP–OTMA (HTMA) complexes have been evaluated from a simulation of the observed fluorescence intensity data. In the induced circular dichroism spectrum, the signal intensity of TSPP in aqueous solutions containing both γ-CD and OTMA has been similar to that containing only γ-CD, suggesting the formation of the 1:1:1 γ-CD–TSPP–OTMA (HTMA) inclusion complex. Capillary electrophoretic study has exhibited the formation of the 1:1 TSPP–OTMA (HTMA) complex, although the 1:2 TSPP–OTMA (HTMA) complex could not be observed, probably because the OTMA (HTMA) concentration used was low. The equilibrium constants for these 1:1 complexes have been evaluated from the variation in the electrophoretic mobility. The equilibrium constant for the formation of the 1:1:1 γ-CD–TSPP–OTMA or γ-CD–TSPP–HTMA complex has been evaluated from a simulation of the electrophoretic mobility change in TSPP solution containing γ-CD and OTMA or HTMA, although the equilibrium constants for the ternary inclusion complexes could not be evaluated using the fluorescence method due to the small fluorescence intensity change.

Introduction

Cyclic oligosaccharides, which have six, seven, and eight D-glucopyranose residues, are called α-, β-, and γ-cyclodextrin (α-, β-, and γ-CD), respectively [1]. They are shaped like a truncated cone with a hollow cavity. The primary and secondary hydroxy groups are positioned at the narrow and wide rim of the CD cavity, respectively. Because lots of hydroxy groups are perched on the ends of the CD cavity, CDs are soluble in water. Due to the relatively hydrophobic cavity of CDs, they include a wide variety of organic compounds to form inclusion complexes in aqueous solution.

The molecular interactions between CDs and water-soluble porphyrin derivatives have been examined by many researchers [2–9]. Tetrakis(4-sulfonatophenyl)porphyrin (TSPP) is one of the most examined porphyrins [5–12]. It has been reported that β-CD is bound to a TSPP molecule from the secondary hydroxy-group side, whereas γ-CD is bound to a TSPP molecule from the primary hydroxy-group side [7].

* Author for correspondence. E-mail: hamai@ipc.akita-u.ac.jp

In aqueous solution, the complexation between an organic cation and an organic anion has been reported for the systems of 1,1′-dimethyl-4,4′-bipyridinium dichloride–Zn TSPP, 1,1′-dimethyl-4,4′-bipyridinium dichloride–Zn tetraphenylporphyrintrisulfonate, and 4,4′,4″,4‴-(21H,23H-porphine-5,10,15,20-tetraryl)tetrakis[1-methylpyridinium] cation dimer–9,10-anthraquinone-2-sulfonate [13–16]. Using spectroscopic procedures, we have examined the complex formation between organic cations and organic anions; the systems of Methylene Blue–naphthalenesulfonates, Methylene Blue–naphthalenedisulfonates, Methylene Blue–2-anthracenesulfonate, Methylene Blue–Acid Orange 7, Methylene Blue–TSPP, Methylene Blue–α-naphthol orange, Methylene Blue–2-naphthol-6-sulfonate, Methylene Blue–1,2-naphthoquinone-4-sulfonate, Thionine–2-naphthalenesulfonate, 1,1′-diheptyl-4,4′-bipyridinium dibromide–tetrakis(4-carboxyphenyl)porphyrin (TCPP), and 1,1′-diheptyl-4,4′-bipyridinium dibromide–hematoporphyrin [17–24]. Capillary electrophoresis has been performed to examine the complex formation of Methylene Blue–2-naphthol-6-sulfonate and Methylene Blue–1,2-naphthoquinone-4-sulfonate [21]. Takayanagi

et al. have investigated the ion association of primary or quarternary alkylammonium ions with aromatic anions such as naphthalenesulfonates, employing capillary electrophoresis [25–27].

Using NMR spectroscopy, Tan *et al*. have revealed that the complexation of γ-CD with an organic anion (2,6-naphthalenedicarboxylate) is greatly enhanced by the addition of an organic cation (2,6-bis(1-pyridiniomethyl)naphthalene dibromide) as a space regulator [28]. The effects of CD have also been investigated for the complexes of Methylene Blue–Acid Orange 7, Methylene Blue–TSPP, Methylene Blue–γ-naphthol orange, Thionine–2-naphthalenesulfonate, 1,1′-diheptyl-4,4′-bipyridinium dibromide–TCPP, and 1,1′-diheptyl-4,4′-bipyridinium dibromide–hematoporphyrin [18–20, 22–24]. Except for the Methylene Blue–TSPP complex, which has been dissociated by the addition of CDs, the formation of ternary inclusion complexes of CD–organic cation–organic anion has been observed. Although the interactions of the organic cation–organic anion complexes with CDs have been examined by means of spectroscopic methods, to our knowledge, there is no capillary electrophoretic study concerning these interactions.

Under the circumstances, we have studied on the complex formation of TSPP with octyltrimethylammonium bromide (OTMA) and hexyltrimethylammonium bromide (HTMA). In addition, the interactions between the organic cation–organic anion complex and γ-CD have been investigated. In this study, we have used capillary electrophoresis as well as absorption, fluorescence, and induced circular dichroism spectroscopy, to examine the physicochemical properties of the complexes among γ-CD, TSPP, and OTMA (HTMA).

Experimental

Absorption, fluorescence, and induced circular dichroism spectra were recorded on a Shimadzu UV-260 spectrophotometer, a Shimadzu RF-540 spectrofluorometer, and a JASCO J-400X spectropolarimeter interfaced to a JASCO DP-500 data processor, respectively. The fluorescence spectra were corrected for the spectral response of the fluorometer. However, the fluorescence spectra in the longer-wavelength region could not fully be corrected, because the sensitivity of the fluorometer in this region was very low. A quartz cell of a 1-cm pathlength was used for the measurements of the induced circular dichroism spectra. Capillary electrophoresis was performed employing a Shimadzu UVmini-1240 spectrophotometer and a Matsusada Precision Devices HCZE-30 PN apparatus as a detector and a high-voltage power supply, respectively. The detection wavelength for TSPP was 412 nm. The applied voltage was maintained at 15.0 kV throughout this study. A GL Science uncoated fused-silica capillary (70.0 cm × 0.05 mm I. D.) was employed for capillary electrophoresis. The effective length of the capillary was 30.0 cm (from an injection end to a detection window). Samples were hydrodynamically injected into the capillary.

The spectroscopic measurements were made at 25 ± 0.1 °C, except for the induced circular dichroism measurements (25 ± 2 °C). The capillary electrophoresis was performed at 25 ± 2 °C.

Tetrakis(4-sulfonatophenyl)porphyrin (TSPP), octyltrimethylammonium bromide (OTMA), and hexyltrimethylammonium bromide (HTMA), which were obtained from Tokyo Kasei Kogyo Co., Ltd. were used as received.

γ-Cyclodextrin (γ-CD), which was purchased from Wako Pure Chemical Industries, Ltd., was used without further purification. Buffers (pH 7.3) of KH_2PO_4 (6.7×10^{-3} M) – Na_2HPO_4 (6.7×10^{-3} M) were employed for spectroscopic and capillary electrophoretic measurements. Concentrations of TSPP were 1.0×10^{-6}, 1.0×10^{-6}, 2.0×10^{-6}, and 1.0×10^{-5} mol dm^{-3} for the absorption, fluorescence, induced circular dichroism, and capillary electrophoretic measurements, respectively.

Results and discussion

Spectroscopic investigation

Complex formation of TSPP with OTMA in aqueous solution

Figure 1 shows Soret absorption spectra of TSPP (1.0×10^{-6} mol dm^{-3}) in aqueous solutions (pH 7.3) containing various concentrations of OTMA. When the OTMA concentration is increased, the absorption peak is very slightly shifted to longer wavelengths (a 2-nm shift at an OTMA concentration of 1.0×10^{-2} mol dm^{-3}), with a reduction of the absorption intensity. A micelle has not been formed, because a critical micelle concentration (CMC) value of OTMA is 1.4×10^{-1} mol dm^{-3} at 25 °C [29]. In the case of TSPP, the absorption intensity of the Q-band is less than one-thirty of that of the Soret band. To avoid the complex behavior caused

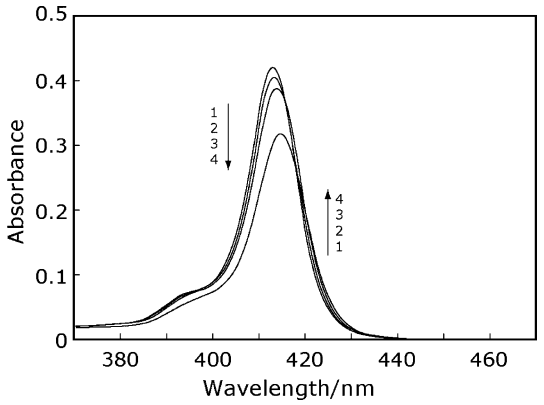

Figure 1. Absorption spectra of TSPP (1.0×10^{-6} mol dm^{-3}) in pH 7.3 buffers containing various concentrations of OTMA. Concentration of OTMA: (1) 0, (2) 1.0×10^{-3}, (3) 3.0×10^{-3}, and (4) 1.0×10^{-2} mol dm^{-3}.

by the dimerization of TSPP at high concentrations of TSPP, we measured only the Soret band. Below about 3×10^{-3} mol dm^{-3} of OTMA, an isosbestic point is observed at 415 nm, although there is no isosbestic point over the OTMA concentration range examined. This finding suggests that 1:1 and 1:2 complexes between TSPP and OTMA are at least formed, although the 1:1 complex predominantly exists at low concentrations of OTMA:

$$\mathrm{TSPP} + \mathrm{OTMA} \overset{K_1}{\rightleftharpoons} \mathrm{TSPP \cdot OTMA} \quad (1)$$

$$\mathrm{TSPP \cdot OTMA} + \mathrm{OTMA} \overset{K_2}{\rightleftharpoons} \mathrm{TSPP \cdot (OTMA)_2} \quad (2)$$

Here, K_1 and K_2 are the equilibrium constants for the formation of the 1:1 TSPP–OTMA complex (TSPP·OTMA) and the 1:2 TSPP–OTMA complex (TSPP·(OTMA)$_2$), respectively.

Figure 2 illustrates fluorescence spectra of TSPP (1.0×10^{-6} mol dm^{-3}) in aqueous solutions (pH 7.3) containing various concentrations of OTMA. Upon the addition of OTMA, the fluorescence intensity is enhanced, accompanied by a very slight shift to shorter wavelengths. This finding indicates the formation of the complex of TSPP with OTMA. The fluorescence intensity change is most likely caused by the decrease in the radiationless rate constant of TSPP in the complex. Above about 5.0×10^{-3} mol dm^{-3} of OTMA, however, the fluorescence intensity was decreased. This is consistent with the result obtained from the absorption spectral change; the 1:2 TSPP–OTMA complex is formed at high OTMA concentrations. In the presence of OTMA, therefore, the fluorescence intensity, I_f, is represented by

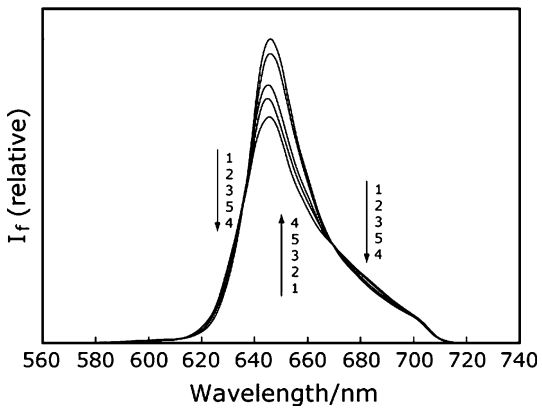

Figure 2. Fluorescence spectra of TSPP (1.0×10^{-6} mol dm^{-3}) in pH 7.3 buffers containing various concentrations of OTMA. The fluorescence intensities were not corrected for the absorbance at the excitation wavelength. Concentration of OTMA: (1) 0, (2) 5.0×10^{-4}, (3) 1.0×10^{-3}, (4) 6.0×10^{-3}, and (5) 1.0×10^{-2} mol dm^{-3}. λ_{ex} = 405 nm.

$$I_f = a[\mathrm{TSPP}] + b[\mathrm{TSPP \cdot OTMA}] + c[\mathrm{TSPP \cdot (OTMA)_2}] \quad (3)$$

where a, b, and c are instrumental constants including the fluorescence quantum yields of TSPP, the 1:1 TSPP–OTMA complex, and the 1:2 TSPP–OTMA complex, respectively. Using K_1 and K_2, the concentrations of the 1:1 and 1:2 TSPP–OTMA complexes are respectively represented as

$$[\mathrm{TSPP \cdot OTMA}] = K_1[\mathrm{TSPP}][\mathrm{OTMA}] \quad (4)$$

and

$$[\mathrm{TSPP \cdot (OTMA)_2}] = K_1K_2[\mathrm{TSPP}][\mathrm{OTMA}]^2 \quad (5)$$

The initial concentration of TSPP, $[\mathrm{TSPP}]_0$, is given by

$$[\mathrm{TSPP}]_0 = [\mathrm{TSPP}] + [\mathrm{TSPP \cdot OTMA}] + [\mathrm{TSPP \cdot (OTMA)_2}] \quad (6)$$

Using Equations (4)–(6), [TSPP] is represented by

$$[\mathrm{TSPP}] = [\mathrm{TSPP}]_0/(1 + K_1[\mathrm{OTMA}] + K_1K_2[\mathrm{OTMA}]^2) \quad (7)$$

Consequently, Equation (3) is rewritten as

$$I_f = (a + bK_1[\mathrm{OTMA}] + cK_1K_2[\mathrm{OTMA}]^2)[\mathrm{TSPP}]_0 / (1 + K_1[\mathrm{OTMA}] + K_1K_2[\mathrm{OTMA}]^2) \quad (8)$$

Figure 3 depicts the observed fluorescence intensity of TSPP as a function of the OTMA concentration, along with the least-squares best fit simulation curve, which has been calculated on the basis of Equation (8). For the best fit simulation curve, the values of K_1, K_2, a, b, and c have been assumed to be 72.0, 170, 3.93×10^7, 1.02×10^8, and 2.25×10^7 mol^{-1} dm^{-3}, respectively (Table 1). For the complexes of TSPP–Methylene Blue, tetrakis(4-carboxyphenyl)porphyrin–1,1'-diheptyl–4,4′-bipyridinium dibromide, and hematoporphyrin–1,1′-diheptyl-4,4′-bipyridinium dibromide, K_1 values have been reported to be 2.35×10^5, 45000 ± 3000, and 1.98×10^5 mol^{-1} dm^3, respectively [19,23,24]. The K_1 value for the TSPP–OTMA complex is two to three orders of magnitude less than the K_1 values for the other complexes containing the porphyrin derivatives. This is probably because the molecular interactions of TSPP with OTMA are weaker than those of the porphyrin derivative with the cationic component (Methylene Blue or 1,1′-diheptyl-4,4′-bipyridinium ion) in the other complexes, due to the absence of an aromatic moiety in OTMA. For the ion association of 1- and 2-naphthalenesulfonates with OTMA, K_1 values have been reported to be 8.1 ± 2.2 (log K_1 = 0.91 ± 0.14)

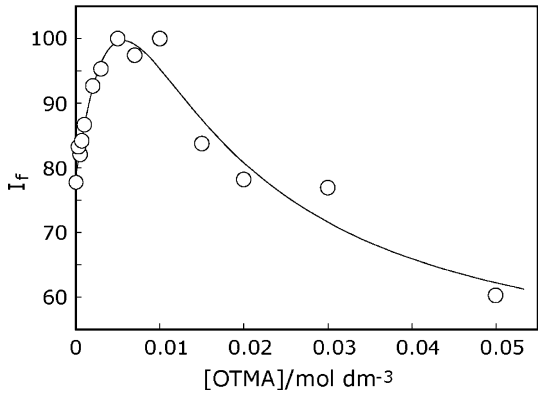

Figure 3. Fluorescence intensities of TSPP (1.0×10^{-6} mol dm^{-3}) in pH 7.3 buffers containing various concentrations of OTMA and the least-squares best fit simulation curve, in which the values of K_1, K_2, a, b, and c have been assumed to be 72, 170, 3.93×10^7, 1.02×10^8, and 2.25×10^7 mol^{-1} dm^3, respectively. λ_{ex} = 420 nm. λ_{obs} = 642 nm.

Table 1. Equilibrium constants for the formation of the 1:1 and 1:2 TSPP–alkyltrimethylammonium bromide complexes (K_1 and K_2), the 1:1:1 γ-CD–TSPP–alkyltrimethylammonium bromide inclusion complex (K_3), and 1:1 γ-CD–TSPP inclusion complex (K_4), which were determined by means of fluorescence spectroscopy and/or capillary electrophoresis

		K_1/mol^{-1} dm^3	K_2/mol^{-1} dm^3	K_3/mol^{-1} dm^3	K_4/mol^{-1} dm^3
Fluorescence	HTMA	98.3	3.40	[a]	1600 ± 200[b]
	OTMA	72.0	170	[a]	1600 ± 200[b]
CE[c]	HTMA	54 ± 2	[d]	47.6[e] 100[f]	1550 ± 30
	OTMA	140 ± 2	[d]	150[e] 349[f]	1550 ± 30

[a]The equilibrium constant could not be estimated.
[b]Ref. 11.
[c]Capillary electrophoresis.
[d]A K_2 value was not obtained, because the 1:2 TSPP–HTMA (OTMA) complex could not be observed by means of capillary electrophoresis.
[e]The K_3 value was evaluated from the simulation, in which the evaluated values of μ_0, μ_1, K_1, and K_4 were used.
[f]The K_3 value was evaluated from the simulation, in which the evaluated values of μ_0, μ_1, μ_2, K_1, and K_4 were used.

and 8.1 ± 1.1 (log K_1 = 0.91 ± 0.07), respectively, which are about ten times less than the K_1 value for TSPP [25].

Complex formation of TSPP with OTMA in γ-CD solution Figure 4 shows absorption spectra of TSPP (1.0×10^{-6} mol dm^{-3}) in aqueous solutions (pH 7.3) containing γ-CD (5.0×10^{-3} mol dm^{-3}) and various concentrations of OTMA. For comparison, Figure 4 also exhibits the absorption spectrum of TSPP in aqueous solution without both γ-CD and OTMA. A red-shift of 2.5 nm in the absorption peak is observed in the presence of only γ-CD. When OTMA is added to a TSPP solution containing γ-CD, the absorption peak is shifted to longer wavelengths, with a reduction of the absorption intensity. A 2-nm shift of the absorption peak to longer wavelengths is observed at an OTMA concentration of 1.0×10^{-2} mol dm^{-3}. Upon the addition of OTMA, the formation of the 1:1 TSPP–OTMA complex is expected at the expense of the 1:1 γ-CD–TSPP inclusion complex. The decrease in the concentration of the γ-CD–TSPP inclusion complex shifts the absorption peak to shorter wavelengths. Taking into account this shorter-wavelength shift of the absorption peak, the observed wavelength shift of 2 nm cannot be explained by the longer-wavelength shift caused by the formation of the TSPP–OTMA complex, because a longer-wavelength shift of only 2 nm has been observed at an OTMA concentration of 1.0×10^{-2} mol dm^{-3} in the absence of γ-CD. Consequently, the above inference suggests that the formation of a ternary inclusion

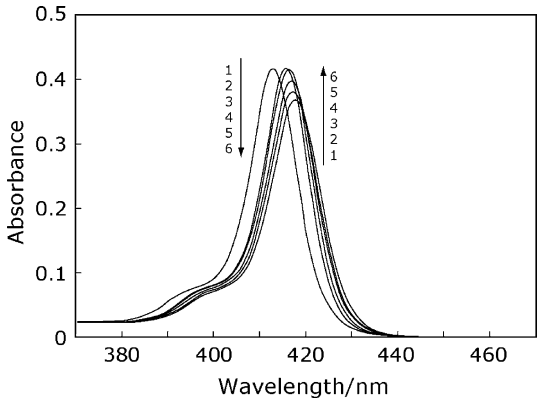

Figure 4. Absorption spectra of TSPP (1.0×10^{-6} mol dm^{-3}) in pH 7.3 buffers containing γ-CD (5.0×10^{-3} mol dm^{-3}) and various concentrations of OTMA, except for curve 1, which is the absorption spectrum in aqueous solution without γ-CD and OTMA. Concentration of OTMA: (1) 0, (2) 0, (3) 1.0×10^{-3}, (4) 3.0×10^{-3}, (5) 5.0×10^{-3}, and (6) 1.0×10^{-2} mol dm^{-3}.

complex of γ-CD with TSPP and OTMA is responsible for the shift of the absorption peak to longer wavelengths.

To confirm the existence of the ternary inclusion complex, we have measured induced circular dichroism (icd) spectra of TSPP (2.0×10^{-6} mol dm^{-3}) in γ-CD (1.0×10^{-2} mol dm^{-3}) solutions with and without OTMA (5.0×10^{-3} mol dm^{-3}) (Figure 5). The icd spectrum of TSPP in pH 7.3 buffer containing γ-CD (1.0×10^{-2} mol dm^{-3}) exhibits a positive band, which is almost the same as that in pH 10.1 buffer (Ref. 11). The signal intensity of the icd spectrum of TSPP in the presence of OTMA is nearly the same as that in the absence of OTMA, indicating that the addition of OTMA induces little or no dissociation of the γ-CD–TSPP inclusion complex. In addition, the icd band is shifted to longer-wavelengths upon the addition of OTMA. These findings indicate that the ternary inclusion complex is formed among γ-CD, TSPP, and OTMA.

$$\gamma\text{-CD} \cdot \text{TSPP} + \text{OTMA} \overset{K_3}{\rightleftharpoons} \gamma\text{-CD} \cdot \text{TSPP} \cdot \text{OTMA} \quad (9)$$

Here, K_3 is the equilibrium constant for the formation of the 1:1:1 γ-CD–TSPP–OTMA inclusion complex (γ-CD·TSPP·OTMA). In the γ-CD–TSPP–OTMA inclusion complex, the γ-CD cavity is most likely to simultaneously accommodate a TSPP molecule and an octyl group of OTMA.

Figure 6 illustrates fluorescence spectra of TSPP (1.0×10^{-6} mol dm^{-3}) in γ-CD (5.0×10^{-3} mol dm^{-3}) solution (pH 7.3) containing various concentrations of OTMA. For comparison, Figure 6 shows the fluorescence spectrum of TSPP in pH 7.3 buffer without both γ-CD and OTMA. When γ-CD is added to a TSPP solution without OTMA, the fluorescence intensity is significantly enhanced, indicating the formation of the γ-CD–TSPP inclusion complex. The enhancement of the fluorescence intensity is most likely caused by the reduction of the radiationless rate constant of TSPP in the inclusion complex. Addition of OTMA (5.0×10^{-3} mol dm^{-3}) to a γ-CD solution of TSPP results in the further enhancement of the TSPP fluorescence, with a slight shift of the fluorescence peak to longer wavelengths. As the OTMA concentration is further increased, the fluorescence intensity is rather reduced. This finding suggests the formation of the γ-CD–TSPP–OTMA ternary inclusion complex, although the 1:2 TSPP–OTMA complex may be formed at high OTMA concentration. At a γ-CD concentration of 5.0×10^{-3} mol dm^{-3}, the observed fluorescence intensity was simulated as a function of the OTMA concentration to estimate the equilibrium constant for the formation of the γ-CD–TSPP–OTMA inclusion complex. However, the variation in the fluorescence intensity was at most 10%, so that the equilibrium constant could not be estimated from the simulation. At an OTMA concentration of 3.0×10^{-3} mol dm^{-3}, we attempted to simulate the observed fluorescence intensity as a function of the γ-CD concentration. As in the case of the simulation as a function of the OTMA concentration, however, the equilibrium constant could not be estimated from the fluorescence intensity change, because the variation of the fluorescence intensity was less than about 10%.

Complex formation of TSPP with HTMA

For HTMA, absorption and fluorescence spectral changes similar to those for OTMA were observed, indicating the formation of the 1:1 and 1:2 TSPP–HTMA complex. The HTMA concentrations used were equal to or less than 1.0×10^{-1} mol dm^{-3}, which was lower than the CMC value of OTMA. Because a CMC value of HTMA is expected to be greater than that of OTMA, HTMA would not form a micelle under our experimental conditions. Using a simulation method, which was applied to the TSPP–OTMA system, K_1 and K_2 values of HTMA were evaluated to be 98.3 and 3.40 mol^{-1} dm^3, respectively. The K_1 value for HTMA is slightly greater than that for OTMA, while the K_2 value for HTMA is two orders of magnitude less than that for OTMA. The reason for the difference in the K_2

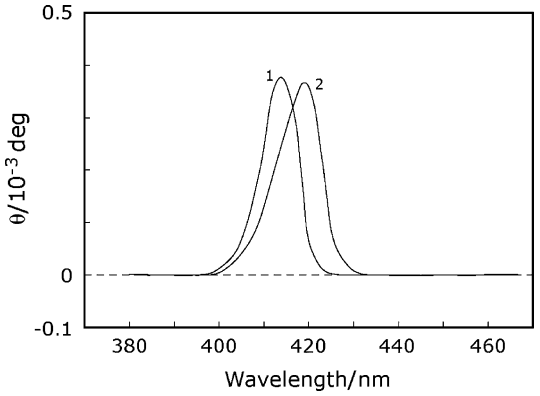

Figure 5. Induced circular dichroism spectra of TSPP (2.0×10^{-6} mol dm^{-3}) in γ-CD (1.0×10^{-2} mol dm^{-3}) solutions (pH 7.3) in the absence and presence of OTMA. Concentration of OTMA: (1) 0 and (2) 5.0×10^{-3} mol dm^{-3}.

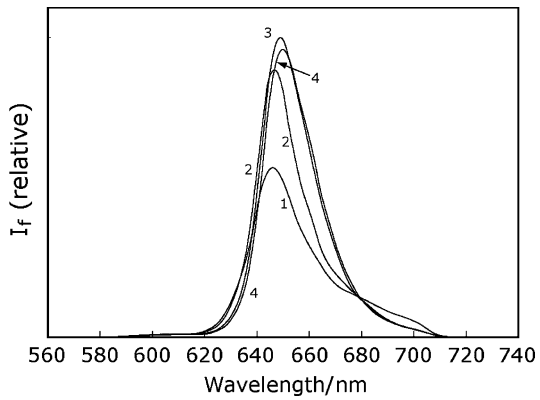

Figure 6. Fluorescence spectra of TSPP (1.0×10^{-6} mol dm^{-3}) in pH 7.3 buffers containing γ-CD (5.0×10^{-3} mol dm^{-3}) and various concentrations of OTMA. For comparison, the fluorescence spectrum of TSPP (1.0×10^{-6} mol dm^{-3}) in pH 7.3 buffers without γ-CD and OTMA is also shown as spectrum 1. Concentration of OTMA: (1) 0, (2) 0, (3) 5.0×10^{-3}, and (4) 1.0×10^{-2} mol dm^{-3}. λ_{ex} = 420 nm.

values for OTMA and HTMA is not clear at present. As one possibility, however, the hydrophobic interactions between two OTMA (HTMA) molecules as well as the interactions between TSPP and OTMA (HTMA) may cooperatively work in the formation of the 1:2 TSPP–OTMA (–HTMA) complex. The cooperative interactions of OTMA seem to be much stronger than those of HTMA, leading to the greater K_2 value for OTMA. In the presence of both γ-CD and HTMA, the absorption and fluorescence spectral changes were similar to those for the γ-CD–TSPP–OTMA system, suggesting the formation of the 1:1:1 γ-CD–TSPP–HTMA inclusion complex. For TSPP solutions containing HTMA and γ-CD, the fluorescence intensity was varied within about 10%. Consequently, the equilibrium constant for the formation of the ternary inclusion complex could not be estimated for the γ-CD–TSPP–HTMA system as well as the γ-CD–TSPP–OTMA system. Thus, we tried to estimate the equilibrium constant for the formation of the 1:1:1 γ-CD–TSPP–OTMA (HTMA) inclusion complex, by means of capillary electrophoresis.

Capillary electrophoretic investigation

Interactions of TSPP with γ-CD and OTMA

Figure 7 shows electropherograms of TSPP (1.0×10^{-5} mol dm^{-3}) in pH 7.3 buffers containing various concentrations of γ-CD. In Figure 7, negative signals at about 170 s are due to an electroosmotic flow (EOF) marker (1-propanol (2 %)). From Figure 7, the electrophoretic mobility of free TSPP, μ_0, is estimated to be -6.18×10^{-4} cm^2 V^{-1} s^{-1} (Table 2). As the γ-CD concentration is increased, the migration time of TSPP is shortened, indicating the formation of the γ-CD–TSPP inclusion complex:

$$\gamma\text{-CD} + \text{TSPP} \overset{K_4}{\rightleftharpoons} \gamma\text{-CD} \cdot \text{TSPP} \qquad (10)$$

where K_4 is the equilibrium constant for the formation of the 1:1 γ-CD–TSPP inclusion complex (γ-CD·TSPP). The incorporation of TSPP into the γ-CD cavity increases the apparent molecular volume of TSPP. The apparently increased volume of a TSPP molecule increases the electrophoretic mobility of TSPP, because TSPP is negatively charged. A K_4 value can be evaluated from the equation concerning the electrophoretic mobility [30]:

$$1/(\mu - \mu_0) = 1/(\mu_2 - \mu_0) + 1/(\mu_2 - \mu_0)K_4[\gamma\text{-CD}]_0 \quad (11)$$

Here, μ and μ_2 are the observed electrophoretic mobility of TSPP and the electrophoretic mobility of the 1:1 γ-CD–TSPP inclusion complex, respectively. Figure 8 shows a plot of $1/(\mu–\mu_0)$ against $1/[\gamma\text{-CD}]_0$ for TSPP in pH 7.3 buffers containing γ-CD. From the plot, K_4 and μ_2 values are evaluated to be 1550 ± 30 mol^{-1} dm^3 and -3.91×10^{-4} cm^2 V^{-1} s^{-1}, respectively (Tables 1 and 2). This K_4 value is identical to a K_4 value for TSPP in pH 10.1 buffer, which has been estimated to be 1600 ± 200 mol^{-1} dm^3 from the fluorescence intensity change [11]. In capillary electrophoresis, the TSPP concentration used is 1.0×10^{-5} mol dm^{-3}, which is

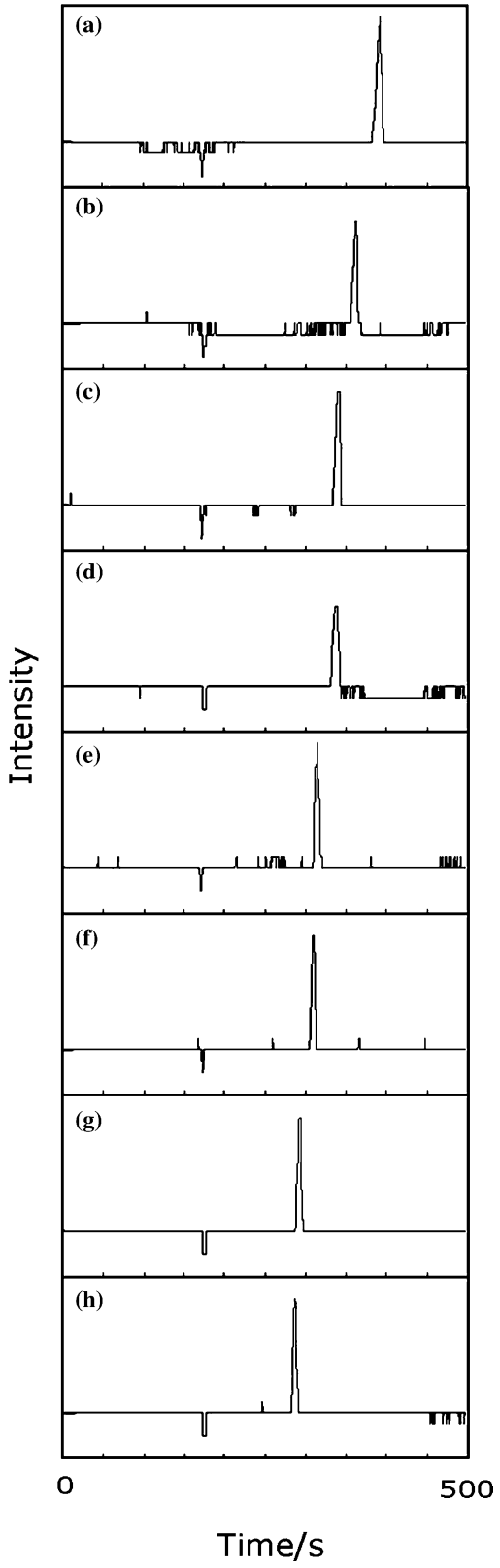

Figure 7. Electropherograms of TSPP (1.0×10^{-5} mol dm^{-3}) in pH 7.3 buffers containing various concentrations of γ-CD. Concentration of γ-CD: (a) 0, (b) 2.0×10^{-4}, (c) 3.0×10^{-4}, (d) 5.0×10^{-4}, (e) 7.0×10^{-4}, (f) 1.0×10^{-3}, (g) 2.0×10^{-3}, and (h) 3.0×10^{-3} mol dm^{-3}. λ_{obs} = 412 nm.

Table 2. Electrophoretic mobilities for free TSPP (μ_0), the 1:1 TSPP–alkyltrimethylammonium bromide complex (μ_1), the 1:1 γ-CD–TSPP inclusion complex (μ_2), and the 1:1:1 γ-CD–TSPP–alkyltrimethylammonium bromide inclusion complex (μ_3)

	$\mu_0/10^{-4}$ cm^2 V^{-1} s^{-1}	$\mu_1/10^{-4}$ cm^2 V^{-1} s^{-1}	$\mu_2/10^{-4}$ cm^2 V^{-1} s^{-1}	$\mu_3/10^{-4}$ cm^2 V^{-1} s^{-1}
HTMA	−6.50	−2.58	−3.91	−1.89[a]
			−3.93[a]	−2.40[b]
OTMA	−6.18	−3.03	−3.91	−1.41[a]
			−3.68[a]	−2.14[b]

[a]The μ_2 and μ_3 values were evaluated from the simulation, in which the evaluated values of μ_0, μ_1, K_1, and K_4 were used.
[b]The μ_3 value was evaluated from the simulation, in which the evaluated values of μ_0, μ_1, μ_2, K_1, and K_4 were used.

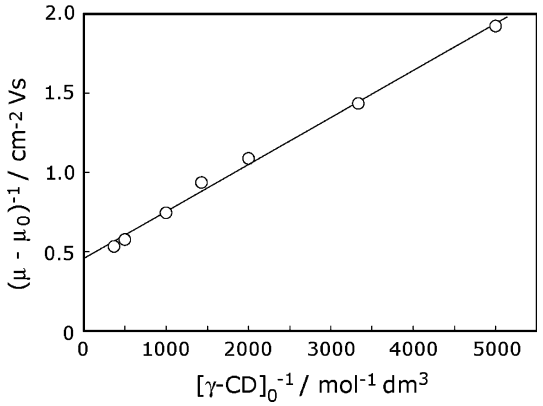

Figure 8. Plot of $1/(\mu-\mu_0)$ against $1/[\gamma\text{–CD}]_0$ for TSPP (1.0×10^{-5} mol dm^{-3}) in pH 7.3 buffers containing various concentrations of γ-CD. λ_{obs} = 412 nm.

higher than that (9.0×10^{-7} mol dm^{-3} (Ref. 11)) used in the fluorescence measurement. Consequently, part of TSPP may dimerize in solution for capillary electrophoresis. In addition to a good straight line shown in Figure 8, however, the result that the same K_4 values have been obtained from the measurements of capillary electrophoresis and fluorescence suggests that the concentration of the TSPP dimer is low relative to that of the TSPP monomer.

With increasing the OTMA concentration, the migration time of TSPP was increased (not shown). However, the migration time of the EOF marker was also lengthened, as the OTMA concentration was increased. As a result, the electrophoretic mobility of TSPP was increased in the presence of OTMA. This implies the formation of the TSPP–OTMA complex. The increase in the migration time of the EOF marker seems to be due to a slight adsorption of OTMA on the capillary surface. On the basis of an equation similar to Equation (11), a K_1 value of TSPP has been evaluated to be 140 ± 2 mol^{-1} dm^3, which is about twice the K_1 value obtained from the simulation of the fluorescence intensity data (Table 1). The reason why the K_1 value obtained from the capillary electrophoresis is greater than that from the fluorescence intensity is not clear at present. The plot for the electrophoretic mobility of TSPP in OTMA solution has given a good straight line (not shown), suggesting that the 1:1 TSPP–OTMA complex is predominantly formed. The absence of the 1:2 TSPP–OTMA complex seems to be mainly due to the experimental conditions of the low OTMA concentrations in the capillary electrophoresis.

In TSPP solution containing OTMA, a μ_0 value for free TSPP and a μ_1 value for the 1:1 TSPP–OTMA complex have been evaluated to be -6.18×10^{-4} and -3.03×10^{-4} cm^2 V^{-1} s^{-1}, respectively. As already noted, a μ_2 value of -3.91×10^{-4} cm^2 V^{-1} s^{-1} has been obtained for the 1:1 γ-CD–TSPP inclusion complex. The magnitude of a μ value depends on both the molecular volume and charge of a chemical species. The smallest μ value (μ_0) for free TSPP is due to the smallest molecular volume of free TSPP among the relevant TSPP species. Although γ-CD has a molecular volume greater than OTMA has, the μ value (μ_2) for the 1:1 γ-CD–TSPP inclusion complex is less than that (μ_1) for the 1:1 TSPP–OTMA complex. In the 1:1 TSPP–OTMA complex, negative charges of TSPP are partly cancelled by a positive charge of OTMA; the 1:1 TSPP–OTMA complex apparently carries a −3 charge, whereas the 1:1 γ-CD–TSPP inclusion complex carries a -4 charge. Although the 1:1 TSPP–OTMA complex has the molecular volume less than that of the 1:1 γ-CD–TSPP inclusion complex, the effect of the negatively small charge of the TSPP–OTMA complex on the μ value surpasses the effect of the molecular volume. This leads to the large μ value of the TSPP–OTMA complex, compared to the γ-CD–TSPP inclusion complex.

Figure 9 illustrates electropherograms of TSPP in γ-CD solution (5.0×10^{-3} mol dm^{-3}) containing various concentrations of OTMA. The migration time of TSPP is lengthened as the OTMA concentration is increased. As in the case of the TSPP–OTMA system, the migration time of the EOF marker is also lengthened. The slight adsorption of OTMA on the capillary surface is likely to be responsible for the increase in the migration time of the EOF marker. In spite of the increase in the migration time of TSPP, the electrophoretic mobility of TSPP is increased with the increase in the OTMA concentration. In the icd study, the formation of the γ-CD–TSPP–OTMA inclusion complex has already been confirmed. In TSPP solution containing both γ-CD and OTMA, therefore, there are free TSPP, the 1:1 TSPP–OTMA complex, the 1:1 γ-CD–TSPP inclusion complex, and the 1:1:1 γ-CD–TSPP–OTMA inclusion complex. In this case, the observed electrophoretic mobility, μ, is represented by

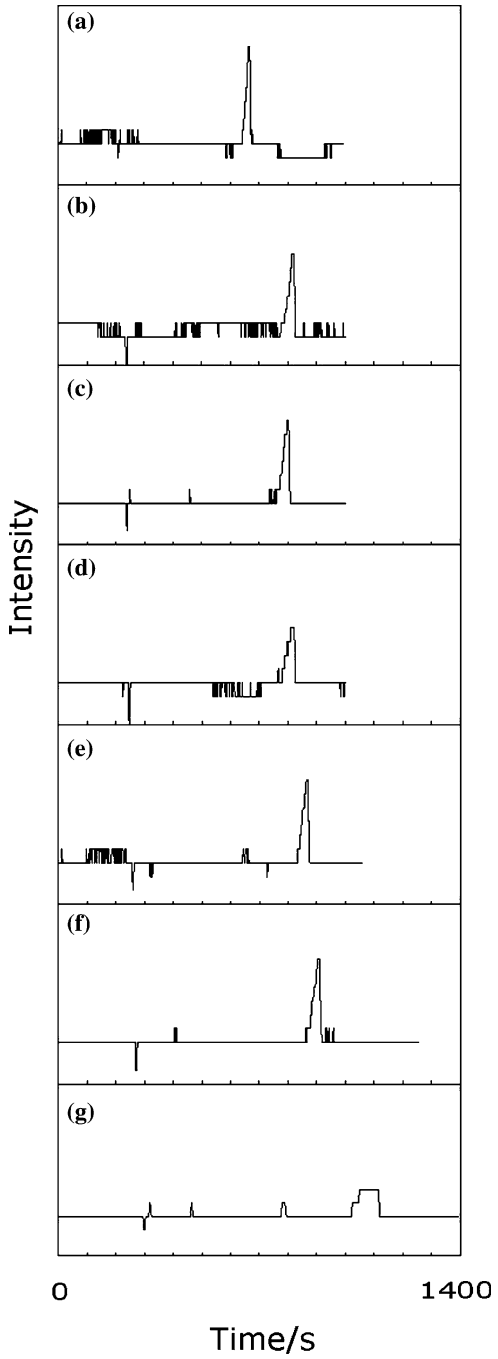

Figure 9. Electropherograms of TSPP (1.0×10^{-5} mol dm^{-3}) in pH 7.3 buffers containing γ-CD (5.0×10^{-3} mol dm^{-3}) and various concentrations of OTMA. Concentration of OTMA: (a) 0, (b) 5.0×10^{-4}, (c) 1.0×10^{-3}, (d) 2.0×10^{-3}, (e) 3.0×10^{-3}, (f) 4.0×10^{-3}, (g) 5.0×10^{-3}, (h) 6.0×10^{-3}, and (i) 7.0×10^{-3} mol dm^{-3}. $\lambda_{obs} = 412$ nm.

$$\mu = (\mu_0 + \mu_1 K_1[\text{OTMA}] + \mu_2 K_4[\gamma\text{-CD}] + \mu_3 K_3 K_4[\gamma\text{-CD}][\text{OTMA}]) / (1 + K_1[\text{OTMA}] + K_4[\gamma\text{-CD}] + K_3 K_4[\gamma\text{-CD}][\text{OTMA}]) \quad (12)$$

Here, μ_3 is the electrophoretic mobility of the 1:1:1 γ-CD–TSPP–OTMA inclusion complex. Figure 10 illustrates the least-squares best fit simulation curve calculated using Equation (12), in which the already evaluated values of μ_0 (-6.18×10^{-4} cm^2 V^{-1} s^{-1}), μ_1 (-3.03×10^{-4} cm^2 V^{-1} s^{-1}), K_1 (140 mol^{-1} dm^3), and K_4 (1550 mol^{-1} dm^3) have been used as the fixed values, whereas μ_2, μ_3, and K_3 have been valuables. From this simulation, values of μ_2, μ_3, and K_3 are evaluated to be -3.68×10^{-4} cm^2 V^{-1} s^{-1}, -1.41×10^{-4} cm^2 V^{-1} s^{-1}, and 150 mol^{-1} dm^3, respectively (Tables 1 and 2). Although a μ_2 value has already been evaluated, we have used a μ_2 value as a parameter in the simulation. In spite of this procedure, the μ_2 value (-3.68×10^{-4} cm^2 V^{-1} s^{-1}) evaluated in the γ-CD–TSPP–OTMA system is close to the μ_2 value (-3.91×10^{-4} cm^2 V^{-1} s^{-1}) evaluated in the γ-CD–TSPP system shown in Figure 7. When the fixed μ_2 value (-3.91×10^{-4} cm^2 V^{-1} s^{-1}) was used in the simulation, the μ_3 and K_3 values were evaluated to be -2.14×10^{-4} cm^2 V^{-1} s^{-1} and 349 mol^{-1} dm^3, respectively, although the fit of the simulation curve was not good compared to the simulation procedure, in which a μ_2 value was used as a parameter.

In the above simulations, the K_1 value, which has been obtained from capillary electrophoresis, has been used. A K_1 value of 72 mol^{-1} dm^3 has been evaluated from the fluorescence intensity change. Thus, we tried to employ a K_1 value of 72 mol^{-1} dm^3 instead of a K_1 value of 140 mol^{-1} dm^3 obtained from the capillary electrophoresis. Values of μ_3 and K_3, which were evaluated in this procedure, were -1.50×10^{-4} cm^2 V^{-1} s^{-1} and 159 mol^{-1} dm^3, respectively. On the other hand, an evaluated μ_2 value was the same as the μ_2 value obtained from the previous simulation. Consequently, a variation in the K_1 value does not influence the other parameters too much.

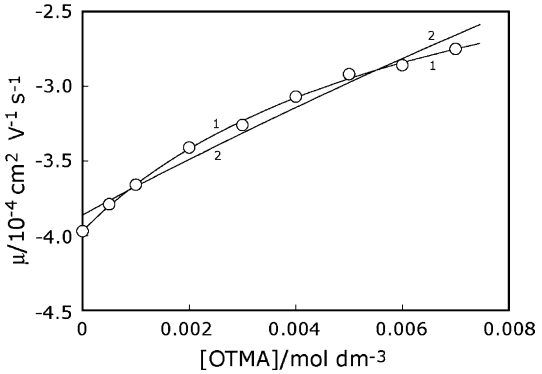

Figure 10. Comparison of the best fit simulation curve for the observed electrophoretic mobility of TSPP (1.0×10^{-5} mol dm^{-3}) in pH 7.3 buffers containing γ-CD (5.0×10^{-3} mol dm^{-3}) and various concentrations of OTMA. Simulation curve 1: the 1:1:1 γ-CD–TSPP–OTMA inclusion complex has been involved in the scheme. The evaluated values of K_1 (140 mol dm^{-3}), K_4 (1550 mol dm^{-3}), μ_0 (-6.18×10^{-4} cm^2 V^{-1} s^{-1}), and μ_1 (-3.03×10^{-4} cm^2 V^{-1} s^{-1}) have been used. The best fit simulation curve 1 has been calculated with $K_3 = 150$ mol^{-1} dm^3, $\mu_2 = -3.68 \times 10^{-4}$ cm^2 V^{-1} s^{-1}, and $\mu_3 = -1.41 \times 10^{-4}$ cm^2 V^{-1} s^{-1}. Simulation curve 2: the 1:1:1 γ-CD–TSPP–OTMA inclusion complex has not been involved in the scheme. The evaluated values of K_1 (140 mol dm^{-3}), K_4 (1550 mol dm^{-3}), and μ_0 (-6.18×10^{-4} cm^2 V^{-1} s^{-1}) have been used. The best fit simulation curve 2 has been calculated with $\mu_1 = 8.23 \times 10^{-4}$ cm^2 V^{-1} s^{-1} and $\mu_2 = -3.56 \times 10^{-4}$ cm^2 V^{-1} s^{-1}.

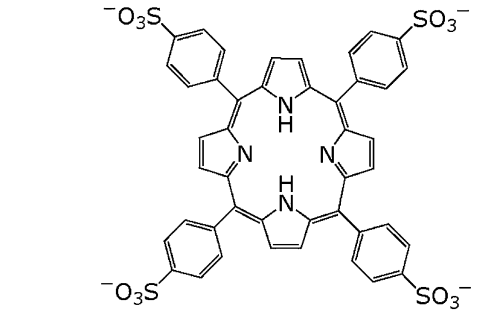

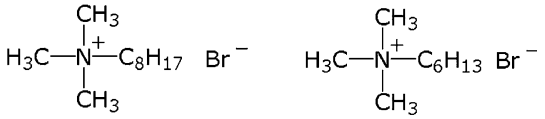

Scheme 1.

When the 1:2 TSPP–OTMA complex was involved in the equilibrium scheme, the best fit simulation curve did not fit the observed data. This result supports the above scheme, in which free TSPP, the 1:1 γ-CD–TSPP inclusion complex, the 1:1 TSPP–OTMA complex, and the 1:1:1 γ-CD–TSPP–OTMA inclusion complex exist in TSPP solution containing γ-CD and OTMA.

To further confirm the existence of the 1:1:1 γ-CD–TSPP–OTMA inclusion complex, we have performed a simulation, in which only the 1:1 γ-CD–TSPP and 1:1 TSPP–OTMA complexes are formed (the γ-CD–TSPP–OTMA inclusion complex is not formed). In this simulation, the values of K_1 (1550 mol^{-1} dm^3), K_2 (140 mol^{-1} dm^3), and μ_0 (-6.18×10^{-4} cm^2 V^{-1} s^{-1}) have been fixed. The best fit simulation curve (curve 2), for which values of μ_1 and μ_2 have been assumed to be 8.23×10^{-4} and -3.56×10^{-4} cm^2 V^{-1} s^{-1}, respectively, does not reproduce the observed data as shown in Figure 10. In addition to the bad fit of the simulation curve to the observed data, the positive μ_1 value is not consistent with the negatively charged species of the 1:1 TSPP–OTMA complex. Consequently, these results confirm the formation of the 1:1:1 γ-CD–TSPP–OTMA inclusion complex in TSPP solution containing γ-CD and OTMA.

Interactions of TSPP with γ-CD and HTMA

As in the case of OTMA, values of K_1 and μ_1 for HTMA have been evaluated to be 54 ± 2 mol^{-1} dm^3 and -2.58×10^{-4} cm^2 V^{-1} s^{-1}, respectively, from the change in the electrophoretic mobility by the addition of HTMA (Tables 1 and 2). This K_1 value for HTMA is 2.6 times less than the K_1 value (140 ± 2 mol^{-1} dm^3) for OTMA. The μ_1 value for HTMA is about 10% greater than that (-3.03×10^{-4} cm^2 V^{-1} s^{-1}) for OTMA, suggesting that the apparent molecular volume of the 1:1 TSPP–HTMA complex is greater than that of the 1:1 TSPP–OTMA complex. However, the molecular volume of HTMA is less than that of OTMA. At present, the reason why the μ_1 value for HTMA is greater than that for OTMA is not clear. The 1:2 TSPP–HTMA complex could not be detected by means of capillary electrophoresis, probably because the HTMA concentration used was low. In capillary electrophoresis of the TSPP–HTMA system, a μ_0 value has been evaluated to be -6.50×10^{-4} cm^2 V^{-1} s^{-1}, which is identical to a μ_0 value (-6.18×10^{-4} cm^2 V^{-1} s^{-1}) obtained in the TSPP–OTMA system, within an experimental error of about 5%.

For the data in capillary electrophoresis of TSPP solution containing γ-CD (5.0×10^{-3} mol dm^{-3}) and various concentrations of HTMA, a simulation similar to that applied to the γ-CD–TSPP–OTMA system was performed using values of K_3, μ_2, and μ_3 as parameters and using the evaluated values of K_1, K_4, μ_0, and μ_1 as the fixed values. As in the case of OTMA, the best fit simulation curve reproduced the observed data (not shown), giving 47.6 mol^{-1} dm^3, -3.93×10^{-4} cm^2 V^{-1} s^{-1}, and -1.89×10^{-4} cm^2 V^{-1} s^{-1} as values of K_3, μ_2, and μ_3, respectively. When the fixed μ_2 value (-3.91×10^{-4} cm^2 V^{-1} s^{-1}) was used in the simulation, the μ_3 and K_3 values were evaluated to be $-2.40 \times 10^{?4}$ cm^2 V^{-1} s^{-1} and 100 mol^{-1} dm^3, respectively. In both simulation procedure, the K_3 value for HTMA is about one third of that for OTMA. Because a short hexyl group of HTMA is less hydrophobic than an octyl group of OTMA is, the interactions of HTMA with TSPP and γ-CD are weak, leading to the smaller K_3 value for HTMA. The μ_3 value for HTMA is less than that for OTMA, suggesting that the ternary inclusion complex containing HTMA is less bulky than that containing OTMA. This is consistent with the fact that the molecular volume of HTMA is less than that of OTMA. The μ_2 value of -3.93×10^{-4} cm^2 V^{-1} s^{-1} for the 1:1 γ-CD–HTMA inclusion complex, which has been evaluated from the ternary system of γ-CD–TSPP–HTMA, is practically identical to that (-3.91×10^{-4} cm^2 V^{-1} s^{-1}) estimated from the binary system of γ-CD–TSPP.

Conclusions

TSPP forms complexes with OTMA and HTMA in pH 7.3 buffers. At high concentrations of OTMA (HTMA), the 1:2 TSPP–OTMA (HTMA) complex is formed besides the 1:1 TSPP–OTMA (HTMA) complex. From the fluorescence intensity changes of TSPP, the equilibrium constants for the formation of the 1:1 and 1:2 TSPP–OTMA (HTMA) complexes have been evaluated. When γ-CD and OTMA are added to TSPP solution, the 1:1:1 γ-CD–TSPP–OTMA inclusion complex is formed.

In capillary electrophoresis, the formation of the 1:1 γ-CD–TSPP inclusion complex has been confirmed. From the variation of the capillary electrophoretic mobility of TSPP with the γ-CD concentration, the equilibrium constant for the formation of the 1:1 γ-CD–TSPP inclusion complex has been evaluated to be 1550 ± 30 mol^{-1} dm^3. Capillary electrophoretic study

exhibits the formation of the 1:1 TSPP–OTMA (HTMA) complex. However, the 1:2 TSPP–OTMA (HTMA) complex could not be detected by means of capillary electrophoresis, because the OTMA (HTMA) concentration used was low. In TSPP solution containing both γ-CD and OTMA (HTMA), the electrophoretic mobility of TSPP has been increased, indicating the formation of the 1:1:1 γ-CD–TSPP–OTMA (HTMA) inclusion complex. For the observed data in capillary electrophoresis of TSPP solution containing both γ-CD and OTMA (HTMA), a simulation has been performed to evaluate the equilibrium constant for the formation of the 1:1:1 γ-CD–TSPP–OTMA (HTMA) inclusion complex.

References

1. W. Saenger: *Angrew Chem. Int. Ed. Engl.* **19**, 344 (1980).
2. H. Hirai, N. Toshima, S. Hayashi and Y. Fujii: Chem. Lett. 643 (1983).
3. J.S Manka and D.S. Lawrence: *Tetrahedron Lett.* **30**, 7341 (1989).
4. J.S. Manka and D.S. Lawrence: *J. Am. Chem. Soc.* **112**, 2440 (1990).
5. S. Mosseri, J.C. Mialocq, B. Perly, and P. Hambright: *J. Phys. Chem.* **95**, 2196 (1991).
6. S. Mosseri, J.C. Mialocq, B. Perly, and P. Hambright: *J. Phys. Chem.* **95**, 4659 (1991).
7. J.M. Ribo, J. Farrera, M.L. Valero, and A. Virgili: *Tetrahedron* **51**, 3705 (1995).
8. K. Kano, N. Tanaka, H. Minamizono and Y. Kawakita: *Chem. Lett.* 925 (1996).
9. K. Kano, R. Nishiyabu, T. Asada, and Y. Kuroda: *J. Am. Chem. Soc.* **124**, 9937 (2002).
10. T. Carofiglio, R. Fornasier, V. Lucchini, C. Rosso, and U. Tonellato: *Tetrahedron Lett.* **37**, 8019 (1996).
11. S. Hamai and T. Koshiyama: *J. Photochem. Photobiol. A: Chem.* **127**, 135 (1999).
12. S. Hamai and T. Koshiyama: *Spectrochim. Acta* A **57**, 985 (2001).
13. M. Rougee, T. Ebbesen, F. Ghetti, and R.V. Bensasson: *J. Phys. Chem.* **86**, 4404 (1982).
14. I. Okura, S. Aono, M. Takeuchi, and Shin Kusunoki: *Bull. Chem. Soc. Jpn.* **55**, 3637 (1982).
15. K. Kano, T. Nakajima, and S. Hashimoto: *J. Phys. Chem.* **91**, 6614 (1987).
16. K. Kano, M. Takei, and S. Hashimoto: *J. Phys. Chem.* **94**, 2181 (1990).
17. S. Hamai: *Bull. Chem. Soc. Jpn.* **58**, 2099 (1985).
18. S. Hamai and H. Satou: *Bull. Chem. Soc. Jpn.* **73**, 2207 (2000).
19. S. Hamai and H. Satou: *Spectrochim. Acta A* **57**, 1745 (2001).
20. S. Hamai and H. Satou: *Bull. Chem. Soc. Jpn.* **75**, 77 (2002).
21. S. Hamai and K. Sato: *Dyes Pigm.* **57**, 15 (2003).
22. S. Hamai: *Bull. Chem. Soc. Jpn.* **73**, 861 (2000).
23. S. Hamai: *Bull. Chem. Soc. Jpn.* **75**, 2371 (2002).
24. S. Hamai: *Supramol. Chem.* **16**, 113 (2004).
25. T. Takayanagi, E. Wada, and S. Motomizu: *Analyst (London)* **122**, 57 (1997).
26. T. Takayanagi, Y. Ohba, H. Haruki, E. Wada, and S. Motomizu: *Anal. Sci.* **14**, 311 (1998).
27. T. Takayanagi, E. Wada, M. Oshima, and S. Motomizu: *Bull. Chem. Soc. Jpn.* **72**, 1785 (1999).
28. W.H. Tan, T. Ishikura, A. Maruta, T. Yamamoto, and Y. Matsui: *Bull. Chem. Soc. Jpn.* **71**, 2323 (1998).
29. M.J. Rosen: Surfactants and Interfacial Phenomena, Wiley, New York, 1989, p. 125.
30. K.L. Rundlett and D.W. Armstrong: *J. Chromatogr. A* **721**, 173 (1996).